Hydrolysis of Wheat Starch and Its Effect on the Falling Number Procedure:

Mathematical Model

Shih-Ying Chang,[1] Stephen R. Delwiche,[2] Nam Sun Wang[1]

[1]*University of Maryland, Department of Chemical Engineering, College Park, Maryland*
[2]*USDA-ARS, Instrumentation and Sensing Laboratory, Building 303, BARC-East, Beltsville, Maryland 20705-2350; e-mail: delwiche@ba.ars.usda.gov*

Received 14 May 2001; accepted 8 March 2002

DOI: 10.1002/bit.10333

Abstract: A population balance model was developed for wheat starch hydrolysis to simulate the performance parameters of a viscosity-based device, known as the Falling Number instrument. The instrument is widely used as an indirect means to gauge the level of preharvest sprout activity in cereal grains such as wheat and barley. The model consists of three competing kinetics: starch gelatinization, enzymatic hydrolysis, and enzyme thermal deactivation. Using established principles of starch rheology and fluid mechanics, the model simulates the velocity profiles of the falling stirrer, starch gel viscosity, and the Falling Number readings at various levels of α-amylase. Model predictions for the velocity of the stirrer at any time during the downward fall, as well as the prediction of the total time needed for the fall, defined as the Falling Number, were in fair agreement with experimental measurements. There was better agreement between the modeled viscosity and the final viscosity of the starch gel as measured by a precision rheometer than there was with the measured Falling Number. © 2002 Wiley Periodicals, Inc.* *Biotechnol Bioeng* **79**: 768–775, 2002.

Keywords: starch; population balance; enzymatic hydrolysis; Falling Number

INTRODUCTION

With starch molecules consisting of very long chains of glucose units connected at carbons 1 and 4 (linear linkage), with occasional branch points at carbons 1 and 6, these molecules, when immersed in water and heated, form pastes and gels that find numerous applications in food and nonfood industries. The physicochemical mechanisms of the starch–water complex formation are well known and were recently summarized (Rao, 1999). Much less is known about the simultaneous action of the kinetic events that explain the viscosity changes that occur in the starch–water complex as it undergoes heating, particularly the influences of granule swelling, gelatinization, enzyme activation (and thermal deactivation), and the hydrolysis of the starch molecules. Kinetic models of enzymatic hydrolysis of starch solutions have been studied for decades. Different theories exist to describe the mode in which gelatinized starch molecules are attacked by enzymes (Thoma, 1976a). The most common theories deal with a random initial attack, followed by multiple attacks (random or endpoint) (Komolprasert and Ofoli, 1991; Thoma, 1976b). All of these proposed models use the distribution-averaged properties of molecules to derive the kinetic schemes. Considering the wide variation in size and weight of starch molecules and most natural polymers, these models are inadequate for describing starch hydrolysis completely. Dean and Rollings (1992) provided certain experimental observations of these distributive characteristics. Analytical data on molecular weights were applied to a set of first-order kinetic equations that modeled the dynamic changes of dextran substrates undergoing enzymatic depolymerization. Analytical data for the molecular weight profiles were used for initial conditions in the solution of a set of discrete equations. The aspect of thermal inhibition of enzymes was not incorporated into their model.

Initiated from crystallization studies, the population balance concept has also been applied to various particulate processes, including suspension and emulsion polymerization, dispersed-phase mixing, and microbial populations. Hunter and Asenjo (1990) proposed a population balance model that described the enzymatic lysis of microbial cells. Taking into account the distributive properties of starch molecules (i.e., the mole-

Correspondence to: Stephen R. Delwiche

Mention of trade names or commercial products in this article is solely for the purpose of providing specific information and does not imply recommendation or endorsement by the U.S. Department of Agriculture or the University of Maryland.

cular weight and chain length distributions), a population model is the most likely procedure for describing the dynamic behavior of starch under enzymatic hydrolysis. An internationally adopted procedure, known as the Falling Number (FN) method, is routinely used throughout the world to characterize the gelatinization and hydrolysis of starch in small grains (e.g., wheat, barley) for the purpose of predicting the product's behavior during industrial processing. Although FN analysis essentially yields a single number (specifically, the time needed for a stirrer rod to descend through a column of cooked meal under a prescribed regimen of heating and stirring), the mechanisms underlying the FN procedure are examples of starch gelatinization and hydrolysis and, as such, are not well understood. Alpha amylase has the effect of decreasing the complex shear modulus and making the flow tendency of the starch paste and gel (as measured by the ratio of the loss modulus to storage modulus) to have increased liquid-like behavior (Champenois et al., 1998). Previous work examined the dynamic nature of the FN procedure by experimental measurement (Chang et al., 1999). The present research explores the rheological behavior of the procedure through mathematical modeling.

The objective of the current research was to develop a model for starch hydrolysis that is based on the population balance of starch molecular weights. General knowledge of starch rheology and basic fluid mechanics is used to quantify the mechanisms of gelatinization and hydrolysis of starch during the FN procedure. The study extends the approach of distributed dynamics of biopolymers such as starch by using a population balance equation as a general model scheme, with consideration given to gelatinization, hydrolysis, and thermal deactivation. A discrete approach is then used to solve the integral-differential equations. Parameters for the fluid system and the macro-molecular model of the starch–water complex are determined experimentally.

MODEL

Assumptions

Operation and experimental observations of an FN measurement were described in Chang et al. (1999). Because of intermittently occurring variations in starch–water behavior, the following assumptions simplified model development:

1. The starch samples are homogeneously mixed and heated during the FN procedure. During the first 60 sec of the procedure the stirring rod is drawn up and down (1 cycle/sec) through the starch–water (7 g : 25 mL) solution contained within a glass test tube of precise diameter (24 mm ID), which, in turn, is immersed in a 100°C water bath. Mechanical agitation ceases at 60 sec when the stirrer is in its highest position, at which time the gel has reached ~75°C and the stirrer descends by force of gravity.

2. The effect of any entrapped air or steam bubbles on stirrer descent velocity is not considered; instead, a smooth falling movement of the stirrer is assumed. Movement was sometimes observed to be absent or even upward (attributed to starch granule swelling and bubble movement) during the first 20 sec after release (Chang et al., 1999).

3. The hydrolysis of starch granules before gelatinization is negligible. This has been checked by comparing the rate constants of pregelatinized and postgelatinized starch (Rollings, 1985).

4. The effect of molecular branching on the overall hydrolysis rate is not significant. This point has been validated by the following experimental observations (Dean and Rollings, 1992):

a) the low proportion of branching, approximately five percent, within a starch molecule, and
b) the minor difference in the hydrolysis rates of branched and unbranched biopolymers.

Adjustment of the kinetic parameters, without changing the reaction mechanisms, can also be applied to accommodate the variations caused by the branching effect.

5. The starch molecules are randomly attacked by α-amylase. Although this has been a long-standing assumption in starch hydrolysis modeling (Thoma, 1976b), it is acknowledged that gylcosidic bonds at the end of the molecule may actually be attacked less frequently than those toward the interior, because in the former case not all the enzyme subsites are binding glycosyl residues. As opposed to starch hydrolysis by glucoamylase, in which glycosidic bonds are broken to release one glucose unit at a time, the hydrolysis reaction by α-amylase is not limited by mass transfer resistance (Sandromán et al., 1996). With the random attack mode assumption, a first-order reaction mechanism is appropriate to describe the segregated kinetics of each polymer fraction (Marc et al., 1983).

Hydrolysis Kinetics

If $g(m,t)$ represents the molecular weight distribution (MWD) of starch at time t, then $g(m,t)dm$ denotes the fraction of molecules with molecular weights between m and $m+dm$ at time t. Changes in the MWD can be described by the following population balance equation around an element of (m, t) space:

accumulation = influx from the depolymerization of large weights − outflux of depolymerization into small weights

This balance gives the following equation:

$$\frac{\partial g(m,t)}{\partial t} = \int_m^\infty 2f(m,m')r(T,t)g(m',t)dm' - r(T,t)g(m,t) \tag{1}$$

where $r(T,t)$ is the depolymerizing rate equation at temperature T and time t that describes the enzymatic hydrolysis kinetics of distributive fractions of polymers. The function $f(m, m')$ is the partition function that describes the probability of enzymatically breaking a starch chain of mass fraction m' into a mass fraction m. Because a random attack is assumed, which implies an equal probability of attacking any glycosidic α (1→4) linkage, a uniform partition function is used for this simulation.

A first-order hydrolysis reaction and a first-order enzyme deactivation are used to describe the specific breakage rate $[r(T,t)]$ of starch polymers and the rate decrease caused by thermal deactivation (Komolprasert and Ofoli, 1991):

$$r(T,t) = c(t)k_0 \exp\left(\frac{-E_a}{RT(t)}\right)n(t): \tag{2}$$

$$\frac{dn(t)}{dt} = -k_{d0}\exp\left(\frac{-E_d}{RT(t)}\right)n(t) \tag{3}$$

Solving Eq. 3 for $n(t)$:

$$n(t) = n_0 \exp\left\{-k_{d0}\int_0^t \exp\left(\frac{-E_d}{RT(\tau)}\right)d\tau\right\} \tag{4}$$

where $c(t)$ is the concentration of gelatinized starch and $n(t)$ is the concentration of active α-amylase with n_0 as the initial value. The parameters E_a and k_0 are the activation energy and kinetic constant of the starch hydrolysis reaction, respectively. E_d and k_{d0} are the activation energy and preexponential constant for enzyme thermal deactivation, respectively, and R is the universal gas constant.

Starch gelatinization kinetics are described by a first-order rate equation, as suggested by many researchers (Cai and Diosady, 1993; Zanoni et al., 1995):

$$\frac{c(t)}{c_0} = 1 - \exp(-k_g t) \tag{5}$$

The rate constant, k_g, is expressed as a function of temperature:

$$k_g(T,t) = k_{g0}\exp\left(\frac{-E_g}{RT(t)}\right) \tag{6}$$

where c_0 is the initial concentration of gelatinized starch, and E_g and k_{g0} are the activation energy and kinetic constant of the gelatinization rate, $k_g(T,t)$, respectively.

Starch Solution Rheology

To relate the MWD to the solution fluid properties, such as intrinsic viscosity, the Mark-Houwink equation is used.

$$[\eta] = kM^a \tag{7}$$

where [η] is the intrinsic viscosity and M is the average molecular weight. Values for the empirical parameters, k and a, were obtained from the literature (Rollings and Thompson, 1984).

The Martin equation, which addresses the theoretical relationship between concentration and viscosity (Rodriguez, 1982), is based on fractional free volume contributions by polymer and solvent:

$$\frac{\eta_{sp}}{c(t)} = [\eta]\exp\{k'[\eta]c(t)\} \tag{8}$$

where k' is a constant empirically fitted from data.

The Arrhenius Law is used to explain the temperature effect on viscosity:

$$\eta = \eta_0 \exp\left(\frac{-E_v}{RT(t)}\right). \tag{9}$$

The specific viscosity η_{sp} is related to the measured viscosity η and the solvent viscosity η_s as follows:

$$\eta_{sp} = \frac{\eta - \eta_s}{\eta_s}. \tag{10}$$

Solution

To solve the integral-differential Eq. [1], a discretization method is used. The primary reasons for the use of this method are: 1) Most available process data for simulations are discrete measurements due to the cycle time limitations from analytical instruments, thus making the discretized approach logical. 2) Once discretized, the population balance changes into a set of differential equations that can be readily integrated by suitable numerical routines.

A method of Hill and Ng (1995) is applied to circumvent the intrinsic problem of intrainterval interactions, that is, when broken daughter fractions still fall into the same discretized bin of the mother fraction. The problem is solved by matching the zeroth and first moments of the original continuous population balance equation with the corresponding two moments of the discretized equations. By doing this the conservation of the total molecular mass is guaranteed.

After discretization, the population balance Eq. [1] becomes N separate ordinary differential equations:

$$\frac{dg_i}{dt} = \sum_{j=i}^{\infty} \beta_j 2 f_j r g_j - \alpha_i r g_i, \quad i = 1, 2, \cdots, N \tag{11}$$

where the correction factors, β_j and α_i, are the probability functions added to account for the intrainterval interactions. For random attack, $\alpha_i = 1/2$ and $\beta_j = 3/4$ (Hill and Ng, 1995).

A geometric size interval is used to divide the whole MWD range into discretized bins. Altogether, this discretization step gave 110 bins ($N = 110$) covering from 400 to 1.5×10^7 g/mol. The upper limit of MWD (1.5×10^7) is determined by integrating the MWD function and selecting the point that covers 99% of all molecular weights. The lower limit of 400 is slightly larger than the molecular weight of maltose (342 g/mol). A Schulz-Zimm distribution function is assumed as the initial MWD function because this distribution is commonly used for describing condensation polymers with a skewed long tail at the high molecular weight end (Dole, 1972):

$$g(m) = \left[\frac{z^z}{M_n \Gamma(z)}\right] \left(\frac{m}{M_n}\right)^z \exp(-zm/M_n) \tag{12}$$

with

$$z = M_n/(M_w - M_n) = 1/(PD - 1) \tag{13}$$

where PD is the polydispersity, which defines the breadth of molecular weight distribution, M_n is the number-average molecular weight, and the gamma function, $\Gamma(z)$, is defined as:

$$\Gamma(z) = \int_0^{\infty} e^{-t} t^{z-1} dt. \tag{14}$$

Rewritten in simpler form, Eq. [12] becomes:

$$g(m) = b^{z+1} \frac{m^z}{z\Gamma(z)} e^{-bm} \tag{15}$$

with:

$$b = \frac{z}{M_n}. \tag{16}$$

where z and M_n are the parameters of the selected MWD function.

The initial molecular weight of wheat starch, with a weight-average molecular weight of 1.7×10^6 g/mol and a polydispersity of 33, was obtained from the literature (Young, 1984), with adjustment of M_w to fit one point of a starch solution of known concentration, temperature, and viscosity. Another commonly used MWD function, the log-normal distribution, was also tested as the initial MWD in a narrower polydispersity range. The simulation results showed that this alternative function did not change the final viscosity results significantly from the Schulz-Zimm function. Instead, the kinetic functions of hydrolysis and enzyme deactivation were the two dominating factors to affect the final viscosity. Because the temperature profile was not the core of this study's scope, empirically fitted exponential equations were used to describe the temperature profiles that were measured experimentally (Chang et al., 1999). A fourth-order Runge-Kutta method was used to solve this set of discretized equations. Programs coded within the MATLAB® environment were developed to conduct the simulations. Values for some of the model parameters, such as E_v, η_0, [η], and k' were determined experimentally, as described in the following section. The rest of the parameters for the model simulations (see Nomenclature) were taken from the literature. Because of the differences between the experimental conditions used in the literature and the conditions applied in the current work, values associated with activation energies and kinetic constants were adjusted to fit one measured viscosity arbitrarily selected from the measurements. These parameters were then applied to simulate the rest of the measured data.

After the dynamic viscosity values of the starch solutions were simulated by the hydrolysis and rheology equations, the final step was to calculate the falling speed profiles from these viscosities. The stirrer's falling movement resembled that of a submerged object through a viscous fluid. For the stirrer, a force balance between gravity F_g and the force associated with the kinetic behavior of the fluid yield the friction factor f for this special flow system (Bird et al., 1960):

$$F_g = A\left(\frac{1}{2}\rho v_\infty^2\right) f, \tag{17}$$

where A is the characteristic area of the tube, ρ is the fluid density, and f is the friction factor (an empirical parameter).

Equation [17] is condensed to

$$f'(\eta, \text{shape}) = \frac{(\text{constant})}{v_\infty^2}. \tag{18}$$

The term v_∞ is the terminal velocity of the stirrer. For a highly viscous fluid possessing a Reynolds number much less than one, such as the starch solution in the present case, terminal velocity is reached within milliseconds (Denn, 1980).

To determine the friction factor f', which is a function of fluid viscosity and the geometry of the submerged object, the stirrer falling speed was measured using a set of carboxyl methyl cellulose (CMC) aqueous solutions with known viscosities, as described in the following section.

$$f' = f_1 \exp(f_2 \cdot \eta) \tag{19}$$

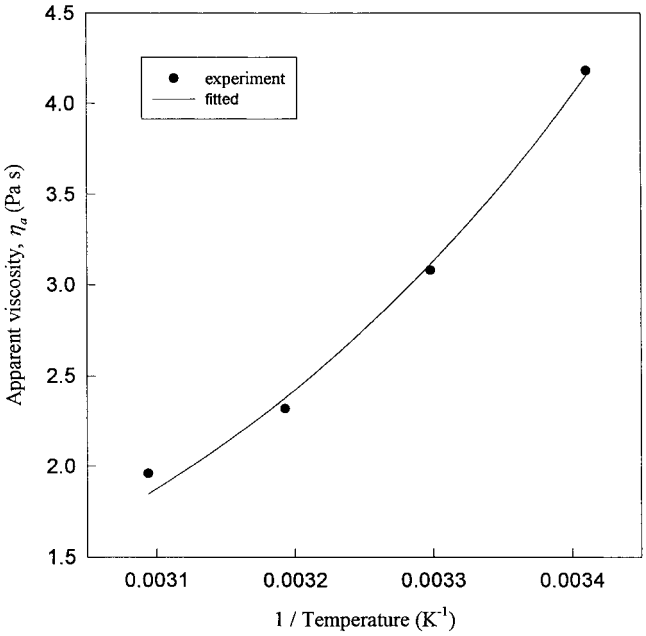

Figure 1. The temperature effect on starch solution viscosity.

EXPERIMENTAL

Estimating E_v, η_0, [η], and k'

Two sets of independent experiments were conducted to determine the parameters needed for the equations of concentration and temperature effects on viscosity (Eqs. 8, 9). Both experiments utilized the MATLAB built-in nonlinear least-square function procedure (LEASTSQ). For the first experiment, the apparent viscosities of a set of wheat starch and water solutions, with fixed concentration and heating procedures, were measured at different temperatures. The viscosities were plotted against the reciprocal temperatures and fitted with an exponential function to get the values of E_v and η_0. Figure 1 shows the Arrhenius Law fitting of the temperature effect on viscosity. It gives the E_v/R value of 2,520 K, which is close to the value of 2,582 K reported by Doublier (1981), measured from wheat starch pastes.

For the second experiment, a set of starch in water solutions with different starch concentrations was measured to fit the parameters of the Martin equation (Eq. 8), namely, the intrinsic viscosity [η] and the constant k'. Figure 2 illustrates the result of $\log(\eta_{sp}/c)$ fitted against c. The offset of the straight line corresponds to $\log[\eta]$ and the slope relates to k' [η]. These fitted values were 1.95 for [η] and 0.10 for Martin's constant k'. These values were close to the reported corresponding values of cellulosic compounds, in which k' ranged from 0.05–0.25 for the cellulose, its derivatives, and certain common synthetic polymers (Ott et al., 1957).

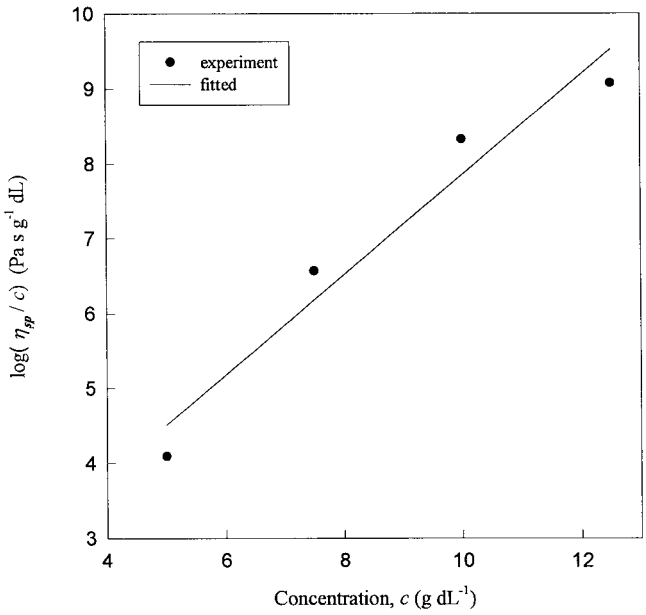

Figure 2. The starch concentration effect on solution viscosity.

Estimating f'

Prepared solutions of carboxy methyl cellulose (CMC) of known viscosity were used with the FN apparatus to determine the friction factor f' (Eq. 19). Figure 3 shows the values of $1/v^2_\infty$ vs. viscosity for the CMC solutions. By a nonlinear least-squares curve fitting operation (MATLAB LEASTSQ), a fitted exponential equation gave the values of f' as a function of viscosity in the specific flow system associated with the FN instrument.

Falling Number Measurement

Details of the FN experiments are provided in Chang et al. (1999). Briefly, 7 g wheat starch (S5127, Sigma Chemical Co., St. Louis, MO), spiked with barley malt

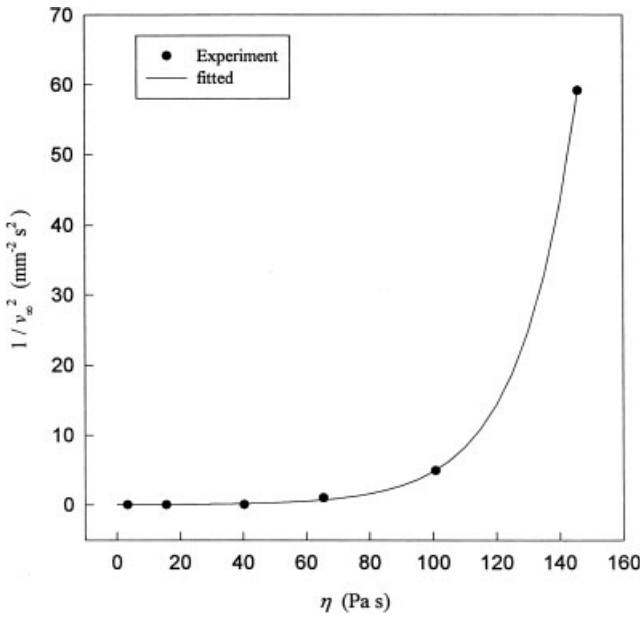

Figure 3. Fitting of the friction factor from carboxymethyl cellulose solutions.

amylase (A2771, Type VIII-A, Sigma), was added to 25 ml distilled water within a precision test tube, whereupon the tube was vigorously shaken several seconds by hand until the starch and water were well mixed. The tube was then immersed in the boiling water bath of the FN instrument. The FN reading was recorded as the time needed, including the 60-sec agitation period, for a geometrically precise stirrer to descend a fixed distance (ca. 65 mm) through the gelatinized starch–water mixture. To represent industrial starch processing conditions, varying levels of barley malt amylase were added to the samples to produce a range in alpha-amylase activity of 400–2,800 IU per liter water. The IU activity scale is patterned after the Nelson-Somogyi reducing sugar procedure (McCleary and Sheehan, 1987). Alpha amylase activity of the wheat starch and malt α-amylase mixture was assayed in triplicate using a commercially available enzyme test kit (Ceralpha method; Megazyme International, Wicklow, Republic of Ireland). Immediately after conclusion of an FN procedure, the viscosity of the paste was measured by a temperature-controlled, parallel plate rheometer (RFS II; Rheometric Scientific, Piscataway, NJ).

RESULTS AND DISCUSSION

The only input for this simulation was the initial level of added α-amylase. The primary output of the model was the viscosity profile of the solution during FN measurement. Two other variables, the stirrer velocity profile and the FN reading, were also determined with the model. Figure 4 illustrates the simulated viscosity profiles with two different enzyme levels added. The solution viscosity increased during the early period of measurement. This was due to the predominant effect of starch gelatinization, with contributions of enzymatic hydrolysis and enzyme thermal deactivation less apparent. This period, in which viscosity increased, explains the delay in downward movement of the stirrer that was observed during actual experimentation (Chang et al., 1999). These effects also determine the maximum viscosity point.

After the maximum viscosity point, the process is dominated by hydrolysis and temperature effects. Because the output from an FN procedure is a single value, the dynamic features of the changing viscosity are not apparent. The predicted final viscosity, corresponding to the final points of the viscosity profiles shown in Figure 4 at different enzyme concentrations, is shown in Figure 5. The predicted values match quite well with the overall trend of the experimental data in the figure.

Figure 6 gives a typical example of the predicted stirrer speed profile. Also shown in this figure are the recorded velocity readings at an enzyme level of 1,610 IU/L. It is seen that the model approximates the same trend as the measured values. The slight lag of the experimental curve can be attributed to the retardation effect of the steam bubbles encountered by the falling stirrer. The bubbles are also thought to have caused the slight degree of nonsmooth velocity behavior from reading to reading, such as those observed around 85 and 110 sec.

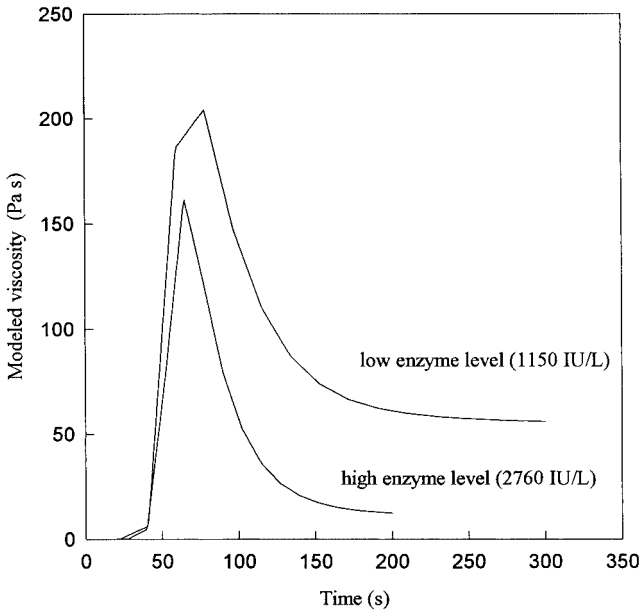

Figure 4. Model simulated viscosity profiles of samples with different levels of α-amylase.

Figure 7 shows the comparison between the modeled and experimental FN readings. Overall, with a standard error of 42 sec, modeled readings were reasonably close to the experimental values. For the range from middle to high levels of added enzyme, the predicted FN readings are close to the measured values. Greater variation

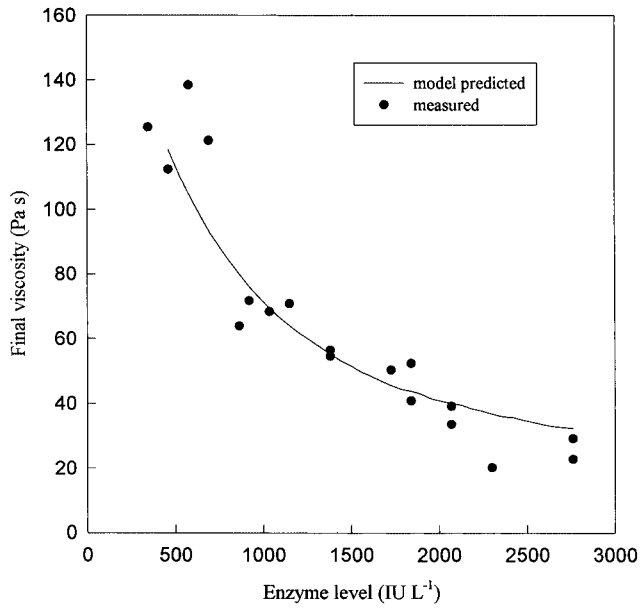

Figure 5. Modeled and measured final viscosities of samples at different levels of α-amylase.

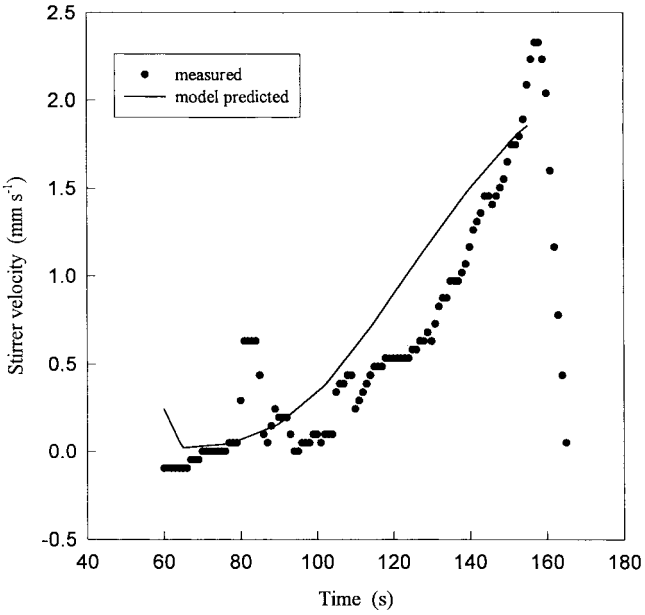

Figure 6. Modeled and measured velocities of the stirrer in a Falling Number instrument.

among the experimental readings at the lower activity levels (< 1,000 IU/L) may be caused by the random occurrences of the steam bubbles impinging on the stirrer. This possibly explains why the instrument manufacturer suggests the best performance of the instrument is around FN readings of 250, which corresponds to the time needed for boiling. Moreover, wheat or barley meal samples with FNs in excess of 400 are seldom observed.

There was a small tendency for the model to underpredict FN at the higher levels of enzyme activity (> 1,400 IU/L). This can be attributed to the reversed flow effect when the stirrer is approaching the bottom of the test tube. Such a reversed flow is more significant when the solution viscosity is low due to a faster upward flow rate. The current model assumes an infinite tube is present. Thus, the effect caused by upward flow of the suspension when the stirrer approaches the bottom of the tube is absent. In the case of high enzyme levels (i.e., lower final solution viscosity), such a condition will result in a slowing down of the stirrer and consequently cause a higher FN reading.

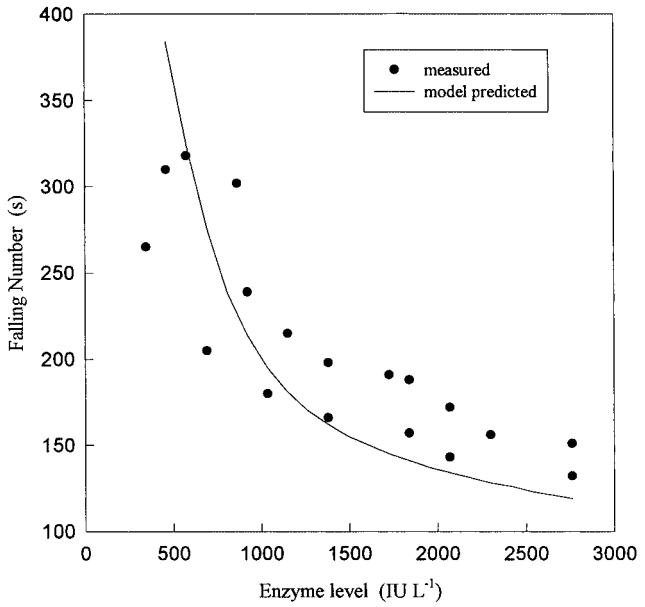

Figure 7. Modeled and measured Falling Numbers of samples with various enzyme levels.

When rheometer final viscosity readings are compared with FN readings (Fig. 5 compared to Fig. 7) with respect to their closeness to measured values, it is seen that the rheometer produced a better agreement. Moreover, the rheometer exhibited slightly better repeatability between runs at a fixed enzyme level. Considering the more tightly controlled conditions of the rheometer, greater precision is expected. However, this should not detract from utility of the FN instrument, recalling the harsher environment in which the instrument is designed to operate. Rather, these findings may provide the basic tools for further improvement of the FN procedure.

SUMMARY AND CONCLUSIONS

A mathematical model was developed to describe the mechanisms underlying starch hydrolysis and their application to the FN measurement. The model consists of several competing processes: starch gelatinization, enzymatic hydrolysis, and thermal deactivation of α-amylase. Based on starch rheology theory, the model is designed to simulate the dynamic viscosity changes, the velocity profile of the falling stirrer, the final viscosity, and the FN reading, given knowledge of the starting enzyme level. A numerical algorithm based on a discretization method was developed to solve the model equations. Confirmed by experimental measurements, the model predicted the instrument behavior and readings reasonably well. Additional investigation into the flow pattern while the stirrer is approaching the tube bottom should improve the agreement between measurements and model predictions.

The model not only provides insight into the FN mechanisms, it also reveals the relative importance of each operating parameter. Therefore, discoveries from this study may lead to further improvements of current methodology or innovative designs of the instrument to enhance the differentiation ability. Considering the analogy between the sample processing conditions used in the FN measurement and common operations in the food processing industry, engineers may benefit from current explorations to optimize and efficiently control those operations.

We thank J. Silverman (University of Maryland, College Park) for early discussions on the molecular weight distribution functions of polymers.

NOMENCLATURE

Variable Properties

Property	Definition
ρ	Fluid density (g mL^{-1})
$[\eta]$	Intrinsic viscosity (g^{-1} dL)
A	Cross-sectional area of test tube (mm^2)
$c(t)$	Concentration of gelatinized starch (g dL^{-1})
c_0	Initial concentration of gelatinized starch (g dL^{-1})
f	Friction factor (dimensionless)
$f(m,m')$	Partition function that describes the probability of enzymatically breaking a starch chain of mass fraction m' into a mass fraction m
F_g	Force of gravity (g mm s^{-2})
f'	Friction factor, working definition (dimensionless)
$g(m,t)$	Molecular weight distribution
$k_g(T, t)$	Gelatinization rate (s^{-1})
M	Average molecular weight (g mol^{-1})
M_n	Number-average molecular weight (g mol^{-1})
M_w	Molecular weight (g mol^{-1})
$n(t)$	Concentration of active α-amylase (IU L^{-1}, where IU = International Unit)
n_0	Initial concentration of active α-amylase (IU L^{-1})
R	The universal gas constant (g mm^2 s^{-2} K^{-1} mol^{-1})
$r(T,t)$	Rate of depolymerization
T	Temperature (K)
t	Time (s)
v_∞	Terminal velocity of stirrer (mm s^{-1})
α_i	Correction factor for population balance equation (dimensionless)
β_j	Correction factor for population balance equation (dimensionless)
η	Measured viscosity (Pa s)
η_s	Solvent viscosity (Pa s)
η_{sp}	Specific viscosity (dimensionless)

Constants

Parameter	Definition, Value (units), Source
a	Parameter for Mark-Houwink equation, 0.68, Rollings and Thompson, 1984; Kurata et al., 1989
E_a	Activation energy for starch hydrolysis, 2.40×10^4 (cal g^{-1} mol^{-1}), Marc et al., 1983
E_d	Activation energy for thermal deactivation, 1.83×10^4 (cal g^{-1} mol^{-1}), Marc et al., 1983
E_g	Activation energy for gelatinization, 3.22×10^4 (cal g^{-1} mol^{-1}), Zanoni et al., 1995
E_v	Activation energy for temperature-dependent viscosity, 5.01×10^3 (cal g^{-1} mol^{-1}), Doublier, 1981 and current work
f_1	Parameter for working friction factor equation, 1.97, Current work
f_2	Parameter for working friction factor equation, 5.5×10^{-3}, Current work
k	Parameter for Mark-Houwink equation, 2.3×10^{-4} (dL g^{-1}), Rollings and Thompson, 1984; Kurata et al., 1989
k_0	Kinetic (rate) constant for starch hydrolysis, 1.4×10^{14} (min^{-1}), Marc et al., 1983
k_{d0}	Preexponential constant for enzyme thermal deactivation, 2.2×10^{11} (min^{-1}), Marc et al., 1983
K_{g0}	Kinetic (rate) constant for gelatinization, 1.0×10^{19} (s^{-1}), Zanoni et al., 1995
k'	Empirical constant for Martin equation, 0.10, Current work
M_n	Number-average molecular weight, 5×10^4, Young, 1984
PD	Polydispersity, 33, Young, 1984

References

Bird RB, Stewart WE, Lightfoot EN. 1960. Transport phenomena. New York: John Wiley & Sons. p 180–207.

Cai W, Diosady LL. 1993. Model for gelatinization of wheat starch in a twin-screw extruder. J Food Sci 58:872–876.

Champenois Y, Rao MA, Walker LP. 1998. Influence of α-amylase on the viscoelastic properties of starch-gluten pastes and gels. J Sci Food Agric 78:127–133.

Chang SY, Delwiche SR, Wang NS. 1999. Hydrolysis of wheat starch and its effect on the falling number procedure: experimental observations. J Sci Food Agric 79:19–24.

Dean SW III, Rollings JE. 1992. Analysis and quantification of a mixed exo-acting and endo-acting polysaccharide depolymerization system. Biotechnol Bioeng 39:968–976.

Denn MM. 1980. Process fluid mechanics. London: Prentice Hall. p 64–67.

Dole M. 1972. The Radiation chemistry of macromolecules, vol. I. New York: Academic Press.

Doublier JL. 1981. Rheological studies on starch—flow behavior of wheat starch pastes. Starch/Stärke 33:415–420.

Hill PJ, Ng KM. 1995. New discretization procedure for the breakage equation. AIChE J 41:1204.

Hunter JB, Asenjo JA. 1990. A population balance model of enzymatic lysis of microbial cells. Biotechnol Bioeng 35:31–42.

Komolprasert V, Ofoli RY. 1991. Starch hydrolysis kinetics of *Bacillus licheniformis* α-amylase. J. Chem Tech Biotechnol 51:209–223.

Kurata M, Tsunashima Y, Iwama M, Kamada K. 1989. Viscosity-molecular weight relationships and unperturbed dimensions of linear chain molecules. In: Brandrup J, Immergut EH, editors, Polymer handbook, 3rd ed. New York: John Wiley & Sons.

Marc A, Engasser JM, Moll, M, Flayeux R. 1983. A kinetic model of starch hydrolysis by α- and β-amylase during mashing. Biotechnol Bioeng 25:481–496.

McCleary BV, Sheehan H. 1987. Measurement of cereal α-amylase: a new assay procedure. Cereal Chem 6:237–251.

Ott E, Spurlin HM, Grafflin MW. 1957. Cellulose and cellulose derivatives. In: Ott E, Spurlin HM, Grafflin MW, editors. High polymers, 2nd ed. New York: Interscience. p 1216–1217.

Rao MA. 1999. Rheology of fluid and semisolid foods: principles and applications. Gaithersburg, MD: Aspen. p 177–218.

Rodriguez F. 1982. Principles of polymer systems. New York: McGraw-Hill. p 167–168.

Rollings JE. 1985. Enzymatic depolymerization of polysaccharides. Carbohydr Polym 5:37–82.

Rollings JE, Thompson RW. 1984. Kinetics of enzymatic starch liquefaction: simulation of the high-molecular-weight product distribution. Biotechnol Bioeng 26:1475–1484.

Sandromán A, Murado MA, Lema JM. 1996. The influence of substrate structure on the kinetics of the hydrolysis of starch by glucoamylase. Appl Biochem Biotechnol 69:329–336.

Thoma JA. 1976a. Models for depolymerizing enzymes: criteria for discrimination of models. Carbohydr Res 48:85–103.

Thoma JA. 1976b. Models for depolymerizing enzymes: application to alpha-amylases. Biopolymers 15:729–746.

Young AH. 1984. Fractionation of starch. In: Whistler RL, BeMiller JN, Paschall EF, editors. Starch: chemistry and technology, 2nd ed. Orlando: Academic Press. p 249–283.

Zanoni B, Peri C, Bruno D. 1995. Modeling of starch gelatinization kinetics of bread crumb during baking. Lebensm-Wiss u-Technol 28:314–318.